Available online at www.sciencedirect.com

SCIENCE DIRECT

Journal of Photochemistry and Photobiology A: Chemistry 182 (2006) 99–106

Journal of Photochemistry and Photobiology A:Chemistry

www.elsevier.com/locate/jphotochem

Photophysical properties of novel cationic naphthalimides

Zsombor Miskolczy [a], József Nyitrai [b], László Biczók [a,*],
Krisztina Sebők-Nagy [a], Tamás Körtvélyesi [c]

[a] Chemical Research Center, Hungarian Academy of Sciences, P.O. Box 17, 1525 Budapest, Hungary
[b] Institute for Organic Chemistry, Budapest University of Technology and Economics, P.O. Box 91, 1521 Budapest, Hungary
[c] Department of Physical Chemistry, University of Szeged, P.O. Box 105, 6701 Szeged, Hungary

Received 19 July 2005; received in revised form 30 January 2006; accepted 31 January 2006
Available online 3 March 2006

Abstract

Novel positively charged naphthalimide derivatives were synthesized, in which *N*-methylpyridinium substituent was attached to the dicarboximide moiety. The absorption and fluorescence spectra were studied, fluorescence lifetimes, fluorescence yields and triplet yields were determined in acetonitrile and CH_2Cl_2. Ion-pairing was found to markedly alter the photophysical properties in the latter solvent. The association with iodide counterion decreased the radiative rate constant. The triplet formation was much more rapid for the 2,3-isomers, whereas the 1,2-derivatives emitted stronger fluorescence. The rate of internal conversion proved to be more than one order of magnitude higher for all *N*-methylpyridinium derivatives compared with that of the parent compounds, which might indicate that the significantly smaller energy gap between the S_1 and S_2 excited states led to more efficient excited state relaxation.

Keywords: Fluorescence; Internal conversion; Intersystem crossing; Excited state; Naphthalimide derivative

1. Introduction

Photoinduced processes of naphthalimides are of particular interest because of their broad-ranging applications in fundamental studies, advanced technology as well as in biological and medical areas. They are capable of initiating the photocleavage of DNA [1–5] and photochemical crosslinking of proteins [6–8]. Irradiation of their brominated derivatives with visible light has been shown to generate photoproducts with strong antiviral activity [9].

Naphthalimides are well-known as promising anticancer agents showing broad-spectrum activity against a variety of human solid tumor cells [10,11]. Several derivatives have reached the phases of clinical trials [12]. Their DNA binding or enzyme inhibitory activity is believed to be pivotal to exert antitumor effect. The dicationic compounds proved to be more potent than the monocationic analogues [13]. 1,8-Naphthalimide linked to dialkylammonium moiety by methylene chain exhibited much stronger association to oligodeoxynucleotides than the neutral molecules due to electrostatic interaction with the phosphate groups [14].

The studies of the photophysical behavior of naphthalimides have contributed to development of new fluorescent probes [15] and optical sensors [16]. The marked change of the fluorescence yield and maximum of 6-(*N*,*N*-dimethylamino)-2,3-naphthalimide with the microenvironment can be implemented for monitoring protein–protein interactions [17]. Dual fluorescence was observed for several substituted-phenyl naphthalimides [18–21] and the relative intensity of the two bands proved to be sensitive to solvent polarity, temperature [22], viscosity [23] and pressure [24]. Some of the monoboronic acid substituted-*N*-phenyl-1,8-naphthalimides displayed remarkable sensitivity and selectivity for saccharides [25].

In the present work, we synthesized novel positively charged naphthalimide derivatives, in which *N*-methylpyridinium substituent is attached to the dicarboximide moiety, and revealed how the location of the dicarboximide group on the naphthalene ring, solvent polarity and counterion affected the rate of the various deactivation pathways of the singlet-excited state. The formulas of the investigated compounds are given in Scheme 1.

---

[*] Corresponding author.
E-mail address: biczok@chemres.hu (L. Biczók).

1010-6030/$ – see front matter © 2006 Elsevier B.V. All rights reserved.
doi:10.1016/j.jphotochem.2006.01.021

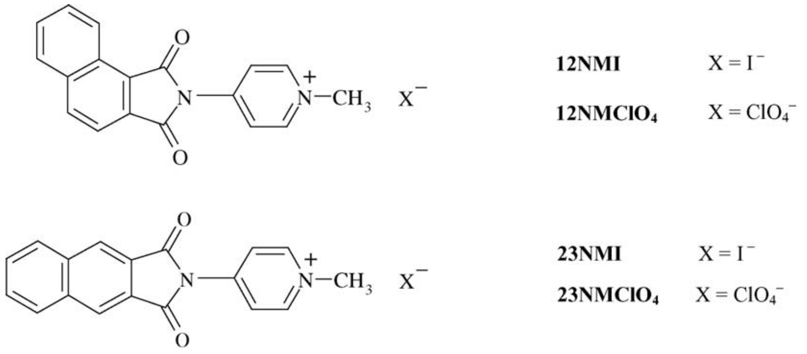

Scheme 1.

2. Experimental details

2.1. Synthesis

IR spectra were obtained on a Zeiss Specord IR 75 spectrometer. ^{1}H NMR (500 MHz) and ^{13}C NMR (125 MHz) spectra were measured on a Bruker DRX-500 spectrometer. Merck precoated Silica gel 60 F_{254} on aluminum sheets were used for qualitative TLC. Spots were detected by UV and phosphomolybdic acid (FMA). Elemental analyses were performed in the Microanalytical Laboratory of the Department of Organic Chemistry, L. Eötvös University, Budapest, Hungary. Melting points were measured on a hot plate melting point apparatus and were uncorrected.

2.1.1. 4-Amino-1-methyl-pyridinium iodide

4-Aminopyridin (95.1 mg; 1.0 mmole) was dissolved in ethyl acetate (3 mL) and methyl iodide (0.25 mL; 4.0 mmole) was added to this solution. Yellow crystals were formed immediately. The reaction mixture was refluxed for 10 min. The crystalline product was filtered off after cooling and washed with dry ether to give 0.22 g (94.4%) of title compound; m.p.: 187–190 °C; literature m.p.: 188–189 °C [26]. IR (KBr): ν 3312 and 3152 (NH_2), 1656, 1544, 1376, 1216, 1200, 832 cm^{-1}. ^{1}H NMR (DMSO-d_6): δ 3,86 (3 H, s, CH_3), 6.79 (2 H, d, J = 7.5 Hz, Ar-3,5-H), 7.98 (2 H, brs, NH_2), 8.10 (2 H, d, J = 7.5 Hz, Ar-2,6-H) ppm.

2.1.2. 4-(1,3-Dioxo-1,3-dihydro-2H-benzo[f]isoindol-2-yl)-1-methylpyridinium iodide (23NMI)

2,3-Naphthalic anhydride, i.e. naphto[2,3-*c*]furan-1,3-dione (0.17 g; 0.85 mmole) and 4-amino-1-methyl-pyridinium iodide (0.20 g; 0.85 mmole) were thoroughly mixed and heated at 200 °C in a sealed tube for 2 h. After cooling and opening the sealed tube the reaction was monitored by TLC (CH_2Cl_2:MeOH, 10:2, Rf_{23NMI} : 0.1, UV/FMA). The starting anhydride was practically consumed. The crude product was refluxed in ethanol (3× 20 mL) and the alcoholic solutions discarded in order to remove the unreacted starting materials. The insoluble product was filtered off and proved to be the pure title compound (0.20 g; 56.5%); m.p. > 294 °C, IR (KBr): ν 1780 and 1736 (CO), 1640, 1512, 1452, 1352, 1240, 848, 784 cm^{-1}. ^{1}H NMR (DMSO-d_6): δ 4.34 (3 H, s, CH_3), 7.87 (2 H, m, Ar-6,7-H), 8.37 (2 H, m, Ar-5,8-H), 8.42 (2H, d, J = 6.5 Hz, Ar-3′,5′), 8.79 (2H, s, Ar-4,9), 9.09 (2H, d, J = 7.0 Hz, Ar-2′,6′) ppm, ^{13}C NMR (DMSO-d_6): δ 47.47 (CH_3), 121.30, 125.71, 125.75, 126.23, 129.67, 130.14, 135.11, 145.77, 146.19, 164.81 (CO) ppm. $C_{18}H_{13}IN_2O_2$ (416.22). Calc. C 51.94, H 3.15, I 30.49, N 6.73. Found C 51.67, H 3.37, I 30.48, N 6.43%.

2.1.3. 4-(1,3-Dioxo-1,3-dihydro-2H-benzo[f]isoindol-2-yl)-1-methylpyridinium perchlorate (23NMClO$_4$)

4-(1,3-Dioxo-1,3-dihydro-2*H*-benzo[*f*]isoindol-2-yl)-1-methylpyridinium iodide (12NMI) (0.10 g; 0.24 mmole) was suspended in 2 mL of water and 70% $HClO_4$ (0.04 mL) was added to this mixture. The suspension was stirred for 1 day. The color of the crystals was changed from pale-yellow into white during this period. The product was filtered off, washed with cold water and ether and dried over P_2O_5 to give the perchlorate salt (90 mg, 96.5%); m.p. > 295 °C, IR (KBr): ν 1776 and 1740 (CO), 1640, 1516, 1240, 1196, 1092, 776 cm^{-1}. ^{1}H NMR (DMSO-d_6): δ 4.37 (3 H, s, CH_3), 7.88 (2 H, m, Ar-6,7-H), 8.38 (2 H, m, Ar-5,8-H), 8.42 (2H, d, J = 6.5 Hz, Ar-3′,5′), 8.80 (2H, s, Ar-4,9), 9.09 (2H, d, J = 7.0 Hz, Ar-2′,6′) ppm. $C_{18}H_{13}ClN_2O_6$ (388.77). Calc. C 55.61, H 3.37, Cl 9.12, N 7.21. Found C 55.57, H 3.16, Cl 8.73, N 6.97%.

2.1.4. 4-(1,3-Dioxo-1,3-dihydro-2H-benzo[e]isoindol-2-yl)-1-methylpyridinium iodide (12NMI)

1,2-Naphthalic anhydride, i.e. naphto[1,2-*c*]furan-1,3-dione (0,70 g; 3.53 mmole) and 4-amino-1-methyl-pyridinium iodide (0.82 g; 3.52 mmole) were thoroughly mixed and heated at 180 °C in a sealed tube for 7 days.

After cooling and opening the sealed tube the crude product was refluxed in ethanol (3× 50 mL) and the alcoholic solutions discarded in order to remove the unreacted starting materials. The insoluble product was filtered off and proved to be the pure title compound (0.82 g; 56.0%); m.p.: 284–286 °C, IR (KBr): ν 1784 and 1724 (CO), 1640, 1512, 1464, 1344, 1272, 832, 784 cm^{-1}. ^{1}H NMR (DMSO-d_6): δ 4.39 (3 H, s, CH_3), 7.87 (1 H, t, J = 7.5 Hz, Ar-7-H[1]), 7.94 (1 H, t, J = 7.5 Hz, Ar-8-H[1]),

---

[1] Interchangeable.

8.08 (1 H, d, J = 8.2 Hz, Ar-6-H^1), 8.29 (1 H, d, J = 8.2 Hz, Ar-9-H^1), 8.44 (2H, d, J = 6.0 Hz, Ar-3′,5′), 8.58 (1 H, d, J = 8.2 Hz, Ar-5-H^1), 8.88 (1 H, d, J = 8.2 Hz, Ar-4-H^1), 9.105 (2H, d, J = 6.0 Hz, Ar-2′,6′) ppm, ^{13}C NMR (DMSO-d_6): δ 47.47 (CH_3), 121.30, 125.71, 125.75, 126.23, 129.67, 130.14, 135.11, 145.77, 146.19, 164.81 (CO) ppm. $C_{18}H_{13}IN_2O_2$ (416.22). Calc. C 51.94, H 3.15, I 30.49, N 6.73. Found C 51.67, H 3.37, I 30.48, N 6.43%.

2.1.5. 4-(1,3-Dioxo-1,3-dihydro-2H-benzo[e]isoindol-2-yl)-1-methylpyridinium perchlorate ($12NMClO_4$)

This compound was similarly prepared to the isomeric perchlorate ($23NMClO_4$) starting with the corresponding iodide (0.62 g; 1.5 mmole) and using 0.25 mL of 70% perchloric acid. Yield: 0.47 g (81.2%); m.p.: 292–297 °C, IR (KBr): ν 1784 and 1728 (CO), 1640, 1516, 1464, 1344, 1272, 1200, 1086, 832, 784 cm^{-1}. ^{1}H NMR (DMSO-d_6): δ 4.35 (3 H, s, CH_3), 7.88 (1 H, t, J = 7.5 Hz, Ar-7-H^1), 7.96 (1 H, t, J = 7.5 Hz, Ar-8-H^1), 8.10 (1 H, d, J = 8.2 Hz, Ar-6-H^1), 8.30 (1 H, d, J = 8.2 Hz, Ar-9-H^1), 8.41 (2H, d, J = 6.0 Hz, Ar-3′,5′), 8.59 (1 H, d, J = 8.2 Hz, Ar-5-H^1), 8.90 (1 H, d, J = 8.2 Hz, Ar-4-H^1), 9.065 (2H, d, J = 6.0 Hz, Ar-2′,6′) ppm, ^{13}C NMR (DMSO-d_6): δ 47.43 (CH_3), 118.66, 120.68, 123.77, 126.30, 126.99, 129.27, 129.43, 130.37, 130.77, 136.27, 136.62, 145.64, 146.27, 165.58 and 166.17 (CO) ppm. $C_{18}H_{13}ClN_2O_6$ (388.77). Calc. C 55.61, H 3.37, Cl 9.12, N 7.21. Found C 55.77, H 3.09, Cl 9.00, N 7.17%.

2.2. Photophysical measurements

Acetonitrile and dichloromethane (Aldrich, HPLC grade) was applied as received. Samples were deoxygenated by purging with nitrogen of high purity. The UV–visible absorption spectra were obtained with a Unicam UV 500 spectrophotometer. Corrected fluorescence spectra were recorded on a Jobin-Yvon Fluoromax-P spectrofluorometer. The energy of the lowest singlet-excited state was derived from the location of the intersection of the normalized absorption and fluorescence spectra. Fluorescence quantum yields were determined relative to that of 9,10-diphenyl-anthracene in cyclohexane, for which a reference yield of 0.90 was taken [27]. Fluorescence lifetimes were measured with time-correlated single-photon counting technique. If the samples did not absorb at 400 nm, an Applied Photophysics SP-3 apparatus with a hydrogen lamp was used. Otherwise, 400 nm light of a Picoquant diode laser (pulse duration 80 ps FWHM) excited the solution and the fluorescence decay was detected with a Hamamatsu R3809U-51 microchannel plate photomultiplier, which was connected to a Picoquant Timeharp 100 electronics. The fluorescence traces were collected until 10^4 counts in the peak channel were reached. Data were analyzed by a non-linear least-squares deconvolution method using Picoquant FluoFit software. The fluorescence decays were described well with single exponential functions. Intersystem crossing quantum yield determinations were carried out by XeCl excimer laser flash photolysis technique using the energy transfer method described in our previous paper [28].

2.3. Calculations

The fully optimized geometry of the ground state of *N*-methylpyridinium naphthalimides in gas phase was calculated by ab initio quantum chemical method at the level of HF/6–31G(d) [29]. The force matrices of the fully optimized structures were found to be positive definite. The energy of the excited states and the oscillator strengths in gas phase were estimated by ZINDO/S CIS method implemented in ORCA [30].

3. Results and discussion

3.1. Absorption spectra

Fig. 1 presents the absorption spectra of the novel cationic naphthalimides, whereas the maxima of the absorption and fluorescence bands are listed together with the energy of the lowest singlet-excited state ($E(S_1)$) in Table 1. For the sake of better comparison, the spectra are normalized with respect to the intense peak in the 31,000–43,000 cm^{-1} range and the spectra of the corresponding unsubstituted naphthalimides are also plotted. The left panels (A and B) show the solvent dependence of the spectra of $12NMClO_4$ and $23NMClO_4$. The first band appears at lower energy for the former compound and exhibits more pronounced vibrational progression for the latter one. Going from CH_2Cl_2 to CH_3CN, a hypsochromic shift is observed, which is larger for the intense peak located in the 33,000–36,000 cm^{-1} domain. The blue-shift of the absorption bands implies that the electron density rearrangement upon excitation makes the solvent–solute interaction weaker in the excited state than in the ground state. The right panels (C and D) in Fig. 1 display how the change of molecular structure affects the absorption properties. The spectra of the *N*-methylpyridinium derivatives are considerably red-shifted compared to those of the unsubstituted naphthalimides suggesting conjugation among the aromatic parts of the molecules. The lower energy bands are identical irrespective of the anion but above 37,000 cm^{-1} the iodide derivatives absorb stronger than the ClO_4^- salts because the first absorption band of I^- is centered at 40,634 cm^{-1} in acetonitrile [31]. Table 1 gives the molar absorption coefficients in acetonitrile. The very low solubility of the studied compounds did not allow the determination of this quantity in CH_2Cl_2.

The ab initio theoretical calculations showed that the naphthalimide moiety was planar and formed 21.1° and 18.5° angle with the plan of the pyridinium ring for 1,2- and 2,3-isomers, respectively. The results of the ZINDO/S CIS calculations are compared with the observed absorption spectra in Figs. 2 and 3. For the 1,2-derivative the calculated excited state energies are ca. 2500 cm^{-1} lower than those expected based on the absorption spectrum. Next to the S_0-S_1 transition two close-lying transitions appear at 29,061 and 29,217 cm^{-1} with oscillator strengths of 0.015 and 0.071, respectively. These transitions correspond to the weak shoulder of the absorption spectrum around 30,400 cm^{-1}. The results of ZINDO/S CIS calculations are in fair agreement with the absorption spectrum for *N*-methylpyridinium 2,3-naphthalimide (Fig. 3). In this case the calculations predict two transitions at 30,390 and 31,367 cm^{-1}

Table 1
Photophysical parameters in acetonitrile and dichloromethane

Solvent	12N	12NMClO$_4$		12NMI		23N	23NMClO$_4$		23NMI	
	CH$_3$CN	CH$_3$CN	CH$_2$Cl$_2$	CH$_3$CN	CH$_2$Cl$_2$	CH$_3$CN	CH$_3$CN	CH$_2$Cl$_2$	CH$_3$CN	CH$_2$Cl$_2$
$\nu_{\max}$ (Absorption) (10^3 cm^{-1})	46.40 (4.576)[a]	46.51 (4.646)	38.99	46.95 4.797)	39.76	46.30 (4.389)[a]	46.30 (3.546)	34.36	47.62 (4.770)	34.54
(log ε (M^{-1} cm^{-1})	39.53 (4.535)[a]	40.00 (4.445)	33.22	40.32 (4.645)	33.33	38.99 (4.765)[a]	35.34 (4.959)	sh 32.15	40.16 (4.617)	sh 32.26
	29.59 (3.437)[a]	34.60 (4.639)	26.88	34.60 (4.654)	27.25	34.60 (3.817)[a]	sh 32.79	28.17	35.34 (4.961)	28.17
		27.78 (3.502)		27.78 (3.499)		29.50 (3.406)[a]	28.65 (3.550)	27.06	sh 32.79	27.10
						28.17 (3.580)[a]	27.47 (3.744)		28.65 (3.563)	
									27.47 (3.739)	
$\nu_{\max}$ (Fluorescence) (10^3 cm^{-1})	22.73[a]	21.60	21.88	21.60	21.88	25.71[a]	sh 25.97	25.91	sh 25.97	25.84
							24.97	24.75	24.97	24.63
$E(S_1)$ (10^3 cm^{-1})	25.53[a]	24.22	24.10	24.10	23.99	27.28[a]	26.88	26.50	26.83	26.47
τ_{F} (ns)	42[a]	43.0 ± 0.5	33.0 ± 0.4	42.5 ± 0.5	29.2 ± 0.3	8.2[a]	6.7 ± 0.2	4.9 ± 0.2	6.3 ± 0.2	4.5 ± 0.2
Φ_{F}	0.77[a]	0.68 ± 0.03	0.59 ± 0.03	0.68 ± 0.03	0.23 ± 0.02	0.27[a]	0.24 ± 0.02	0.20 ± 0.02	0.24 ± 0.02	0.089 ± 0.004
Φ_{ISC}	0.24[a]	0.06 ± 0.01	0.17 ± 0.02	0.04 ± 0.01	0.22 ± 0.03	0.70[a]	0.49 ± 0.05	0.43 ± 0.05	0.42 ± 0.04	0.45 ± 0.05
Φ_{IC}	Negligible[a]	0.26 ± 0.04	0.24 ± 0.04	0.28 ± 0.04	0.55 ± 0.04	0.03[a]	0.27 ± 0.05	0.37 ± 0.05	0.34 ± 0.05	0.46 ± 0.05
k_{F} (10^6 s^{-1})	18[a]	16 ± 1	18 ± 1	16 ± 1	7.9 ± 0.7	33[a]	36 ± 3	41 ± 3	38 ± 4	20 ± 2
k_{ISC} (10^6 s^{-1})	6[a]	1.4 ± 0.3	5.1 ± 0.7	0.9 ± 0.3	7.5 ± 1.0	85[a]	73 ± 8	88 ± 11	67 ± 7	100 ± 12
k_{IC} (10^6 s^{-1})	Negligible[a]	6.0 ± 1.0	7.2 ± 1.2	6.6 ± 1.0	19 ± 2	4[a]	40 ± 8	76 ± 11	54 ± 8	100 ± 12

[a] Ref. [33], the log ε values given in parenthesis were measured in the absorption maxima of the *N*-methyl derivative; sh indicates shoulder.

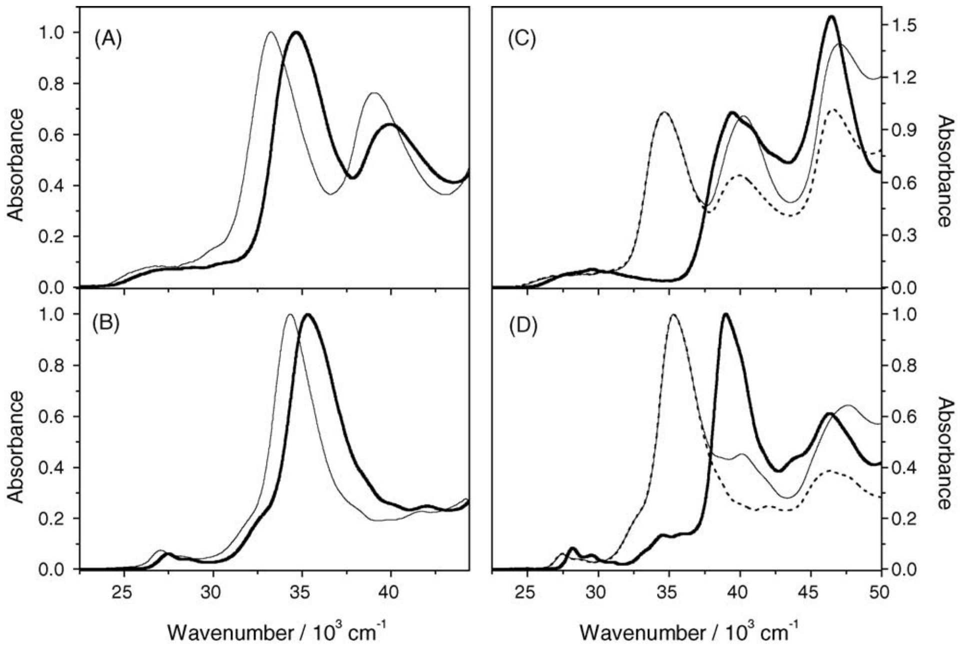

Fig. 1. Solvent effect on the absorption spectra for $12NMClO_4$ (A) and $23NMClO_4$ (B); in CH_2Cl_2 (thin line) and CH_3CN (heavy line). Absorption spectra in acetonitrile for 12NMI (thin line), $12NMClO_4$ (dash line), 1,2-naphthalimide (heavy line) (C) and for 23NI (thin line), $23NClO_4$ (dash line), 2,3-naphthalimide (heavy line) (D).

with very low (ca. 0.002) oscillator strengths. The transition at 33,728 cm^{-1} has 0.034 oscillator strengths and seems to be related to the shoulder around 32,500 cm^{-1}. It is worth noting that the energy gap between the first absorption band (band 1) and the second absorption band appearing as a shoulder (band 2) is significantly larger for the *N*-methylpyridinium naphthalimides than that reported for the *N*-phenyl derivatives [18]. Previous papers on several substituted-phenyl derivatives of naphthalimides demonstrated that the relative position of band 1 and 2 governed the rate of internal conversion [18–20]. The relaxation via the torsion of the substituted-phenyl moiety and solvent reorientation was suggested to lower the energy difference between these states. Based on the solvent and substituent effects on the absorption spectra, bands 1 and 2 were attributed to ππ* and nπ* transitions, respectively. This assignment may be also valid for *N*-methylpyridinium naphthalimides because their spectral characteristics closely resemble that published for the substituted-phenyl derivatives [18–20].

3.2. Fluorescence spectra

Fig. 4 demonstrates that the fluorescence spectra of both the 1,2- and 2,3-isomers of *N*-methylpyridinium naphthalimides are markedly red-shifted relative to those of the unsubstituted derivatives and no anion effect is observed in acetonitrile. The replacement of this solvent with CH_2Cl_2 causes minor

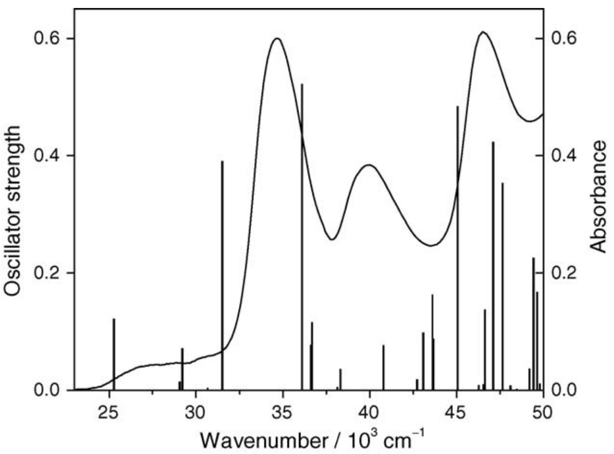

Fig. 2. Comparison of the transition energies and oscillator strengths calculated by ZINDO/S method (vertical lines) with the absorption spectrum of $12NMClO_4$ in acetonitrile.

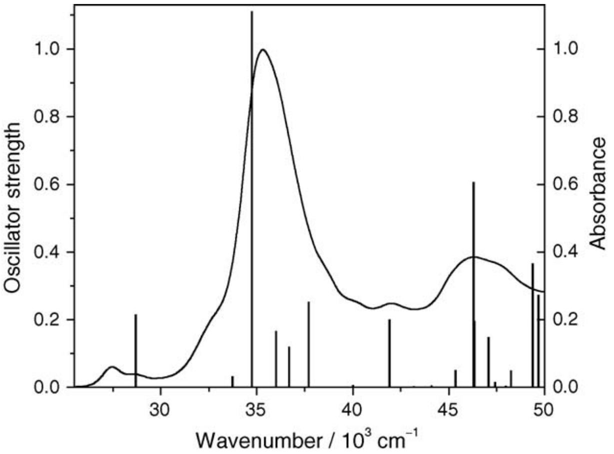

Fig. 3. Comparison of the transition energies and oscillator strengths calculated by ZINDO/S method (vertical lines) with the absorption spectrum of $23NMClO_4$ in acetonitrile.

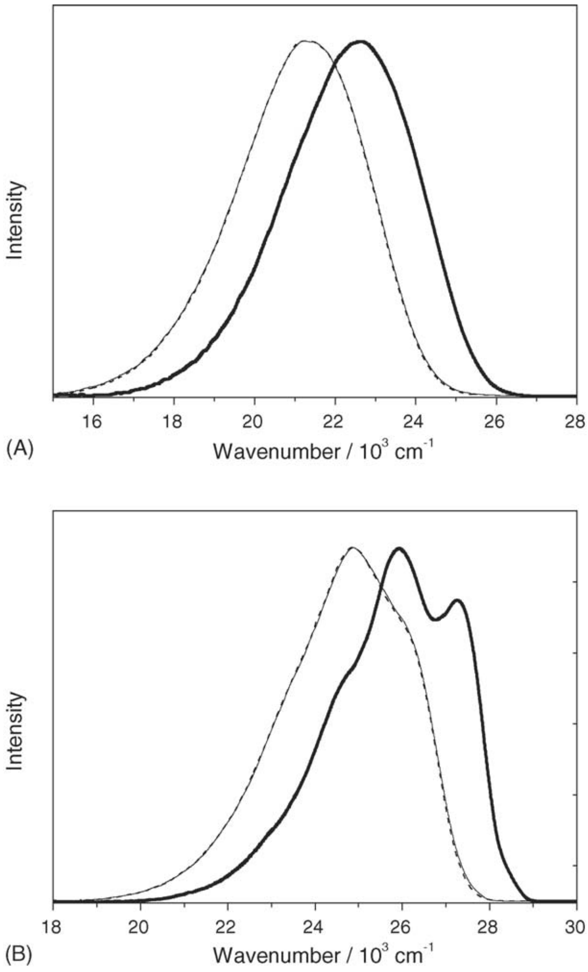

Fig. 4. Fluorescence spectra for 12NMI and $12NMClO_4$ (dash line), unsubstituted 1,2-naphthalimide (heavy line) (A); 23NMI and $23NMClO_4$ (dash line), unsubstituted 2,3-naphthalimide (heavy line) (B) in acetonitrile.

spectral alterations except the more pronounced vibronic structure evolution for the fluorescence band of $23NMClO_4$ and 23NMI. The fluorescent behavior of the studied compounds is entirely different from that reported for the corresponding *N*-phenyl derivatives. Dual fluorescence was found in the case of *N*-phenyl-2,3-naphthalimide [23]. The higher energy band was attributed to a conformer in which the phenyl moiety and the naphthalimide skeleton are orthogonal to each other, whereas the fluorescence at long wavelength was shown to originate from a singlet-excited state of coplanar structure, which was stabilized by the extended conjugation [18]. *N*-Phenyl-1,2-naphthalimide emitted only long-wavelength fluorescence with very low quantum yield peaking at 16,529 cm^{-1} in acetonitrile [18]. The fluorescence maximum is located at much higher energy (21,360 cm^{-1}) for $12NMClO_4$ and 12NMI. The fluorescence band of $23NMClO_4$ and 23NMI exhibits even smaller (ca. 1500 cm^{-1}) Stokes shift implying slight structural change upon excitation. The lack of the low-energy fluorescence band for all compounds studied now probably indicates that the positive charge of the *N*-methylpyridinium moiety precludes the development of the extended conjugation of the aromatic π-electrons.

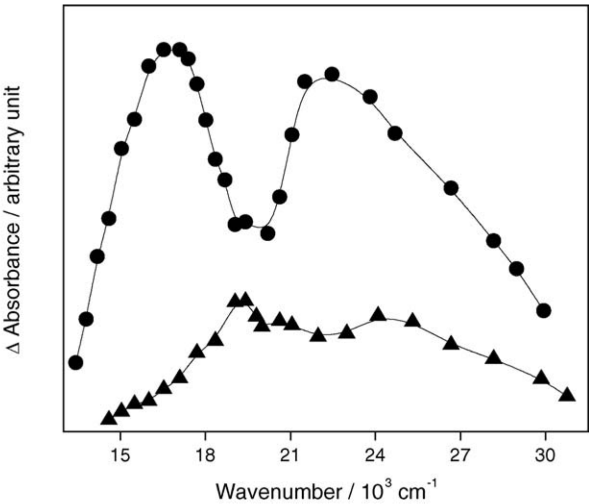

Fig. 5. Absorbance change at various wavenumbers recorded immediately after laser flash for $23NMClO_4$ (circles) and $12NMClO_4$ (triangles) in CH_2Cl_2.

3.3. Triplet formation

Flash photolysis of *N*-methylpyridinium naphthalimide solutions with excitation at 308 nm from an excimer laser gave short-lived species with absorption build up within the duration of the laser pulse and decay on the 10 μs time scale. The transient absorption spectra recorded after the complete decay of the fluorescence signal are presented in Fig. 5 for 30 μM $12NMClO_4$ and 20 μM $23NMClO_4$ in CH_2Cl_2. The spectra, which were independent of the anion and solvent, were assigned to absorption of triplet-excited species based on the following arguments: (i) in the presence of oxygen the transients were quenched and (ii) addition of perylene shortened the decay time of the transient and concomitant formation of triplet perylene was observed. The well-established triplet perylene absorption at 490 nm [32] and the efficient triplet sensitization by naphthalimides was exploited to determine the triplet yield (Φ_{ISC}) with the method described in a previous paper [28]. The rate of the energy transfer was diffusion controlled ($k_q > 3 \times 10^9\ M^{-1}\ s^{-1}$) indicating that the triplet energy for all naphthalimides studied is higher than that of perylene (148 kJ mol^{-1}) [32].

3.4. Effect of hydroxylic solvents

The studied compounds proved to be unstable in the presence of hydroxylic compounds even in the ground state. As a representative example, Fig. 6 shows the alteration of the absorption spectra after addition of 1 M methanol in acetonitrile. The insets display the time dependence of the absorbances and the curves give the results of the non-linear least-squares fit assuming pseudo-first order reaction kinetics. The calculated rate constants for the dark reactions are 0.014 and 0.010 min^{-1} in the case of $23NMClO_4$ and $12NMClO_4$, respectively. Because of the decomposition of *N*-methylpyridinium naphthalimides in hydroxylic media in the absence of irradiation further studies have been performed in aprotic solvents.

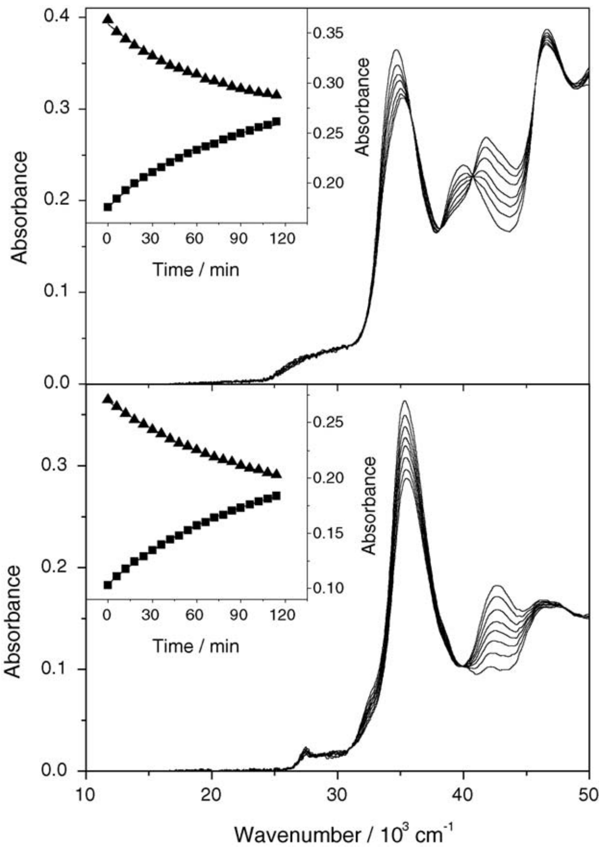

Fig. 6. Alteration of the absorption spectra of $12NMClO_4$ (upper panel) and $23NMClO_4$ (lower panel) after addition of 1 M methanol in acetonitrile. Insets present the absorbance changes in the function of time at 34,480 cm^{-1} (triangles) and 42,550 cm^{-1} (squares).

3.5. Photophysical parameters

Fluorescence lifetimes and the quantum yields of the deactivation processes of the singlet-excited state were measured in acetonitrile and dichloromethane. In less polar solvents, such as e.g. toluene and hexane, the determination of these quantities was precluded by the negligible solubility. It is apparent from Table 1 that the lifetime (τ_F) and the quantum yield of fluorescence (Φ_F) always diminish when acetonitrile solvent is replaced by dichloromethane. At the same time, the quantum yield of triplet formation (Φ_{ISC}) significantly increases for 1,2-derivatives, and remains practically unchanged for 2,3-derivatives. When ClO_4^- is substituted for I^-, the photophysical properties barely alter in acetonitrile. On the other hand, in the case of the 1,2-isomers in CH_2Cl_2, the quantum yields of internal conversion (Φ_{IC}) increases with a concomitant diminution of the fluorescence lifetime and quantum yield. The largest anion dependence for the 2,3-isomers appears in the fluorescence yield, which decreases by more than factor of two in CH_2Cl_2. These effects probably stem from ion-pairing. In polar solvents, such as CH_3CN, the ions are dissociated and therefore, the counterion marginally affects the singlet-excited state depopulating processes. However, in a less polar solvent the weaker solvent–solute interactions expedite the association of the oppositely charged ions by Coulomb attraction. The photophysical characteristics strongly vary with the location of the substituent on the naphthalene ring, as it has been also observed for 12N and 23N. For the sake of comparison, Table 1 also gives the parameters of the unsubstituted 1,2- and 2,3-naphthalimides (12N and 23N) taken from a previous paper [33]. The most substantial difference is seen in the quantum yield of internal conversion (Φ_{IC}), which is greatly enhanced by the covalent linking of an *N*-methylpyridinium group to the imide moiety. However, introduction of this group leads to much smaller increase in Φ_{IC} than reported for *N*-phenyl derivatives [18].

3.6. Rate constants of excited state deactivation

In order to reveal how the counterion, solvent polarity and the molecular structure influence the competition between the various energy dissipation channels of the lowest singlet-excited state, the rate constants for fluorescence emission (k_F), intersystem crossing (k_{ISC}) and internal conversion (k_{IC}) were derived using the expressions given below:

$$k_F = \frac{\Phi_F}{\tau_F} \tag{1}$$

$$k_{ISC} = \frac{\Phi_{ISC}}{\tau_F} \tag{2}$$

$$k_{IC} = \frac{1 - \Phi_{ISC} - \Phi_F}{\tau_F} \tag{3}$$

The results displayed in Table 1 demonstrate that the N-substitution with a methylpyridinium moiety brings about at least one order of magnitude rise in the rate constant of internal conversion. Lim established that the close-neighboring excited states induce efficient radiationless deactivation via vibronic interaction [34]. Thus, the more rapid internal conversion of methylpyridinium naphthalimides might arise from the smaller energy difference between the S_1 and S_2 states.

The *N*-methylpyridinium derivatives possess much longer fluorescence lifetime and much higher fluorescence quantum yield than the values reported for *N*-phenyl naphthalimides [18]. This fact is attributed to the slower internal conversion, which in turn, arises from the weaker vibronic coupling and larger energy gap between the S_1 and S_2 states in the case of the former compounds.

The radiative rate constant exhibits marginal change upon substitution with an *N*-methylpyridinium moiety irrespective of the counterion in acetonitrile. However, significantly lower value is obtained for the iodide salts in CH_2Cl_2. The dissimilarity of k_F for the ClO_4^- and I^- derivatives in CH_2Cl_2 may be due to the larger charge transfer character in the ion-pairs formed in this less polar solvent when the compounds contain the latter, easier oxidizable and polarizable anion. As Gould et al. pointed out [35,36] based on a theoretical model, the increase of the charge transfer character of a complex results in a gradual diminishment of its radiative rate constant. The yellow color of 12NMI and 23NMI crystals also indicates charge transfer type interaction between the ions because $12NMClO_4$ and $23NMClO_4$ are white in solid phase.

The rate constant of triplet formation (k_{ISC}) is mainly governed by the relative positions of the singlet and triplet energy levels. As the k_{ISC} values are much larger for the 2,3-naphthalimides, they are less sensitive to the changes in counterion and solvent polarity than k_{ISC} of the 1,2-isomer.

Acknowledgements

The support of this work by the Hungarian Scientific Research Fund (OTKA, Grant T049645) and by the 1/A/005/2004 NKFP MediChem2 Project are very appreciated. The authors are also indebted to Dr. Áron Szöllőssy for his contribution by measuring NMR spectra, and K. Ófalvi for recording IR spectra. Our thanks go to H. Medzihradszky-Schweiger for performing microanalysis.

References

[1] J.E. Rogers, B. Abraham, A. Rostkowski, L.A. Kelly, Photochem. Photobiol. 74 (2001) 521.
[2] J.E. Rogers, S.J. Weiss, L.A. Kelly, J. Am. Chem. Soc. 122 (2000) 427.
[3] B.M. Aveline, S. Matsugo, R.W. Redmond, J. Am. Chem. Soc. 119 (1997) 11785.
[4] I. Saito, M. Takayama, H. Sugiyama, K. Nakatani, J. Am. Chem. Soc. 117 (1995) 6406.
[5] I. Saito, M. Takayama, S. Kawanishi, J. Am. Chem. Soc. 117 (1995) 5590.
[6] J. Zhang, J. Woods, P.B. Brown, K.D. Lee, R.R. Kane, Bioorg. Med. Chem. Lett. 12 (2002) 853.
[7] M.F. Braña, J.M. Castellano, M. Moran, M.J. Perez de Vega, X.D. Qian, C.A. Romerdahl, G. Kellhauer, Eur. J. Med. Chem. 30 (1995) 235.
[8] B. Abraham, L.A. Kelly, J. Phys. Chem. B 107 (2003) 12534.
[9] T.C. Chanh, D.E. Lewis, M.M. Judy, F. Sogandares-Bernal, G.R. Michalek, R.E. Utecht, H. Skiles, S.-C. Chang, J.L. Matthews, Antiviral Res. 25 (1994) 133.
[10] C. Bailly, C. Carrasco, A. Joubert, C. Bal, N. Wattez, M.-P. Hildebrand, A. Lansiaux, P. Colson, C. Houssier, M. Cacho, A. Ramos, M.F. Braña, Biochemistry 42 (2003) 4136 (and references therein).
[11] M.F. Braña, A. Ramos, Curr. Med. Chem. Anti-Cancer Agents 1 (2001) 237.
[12] V.K. Malvyiya, P.Y. Liu, D.S. Alberts, E.A. Surwitt, J.B. Craig, E.V. Hanningan, Am. J. Clin. Oncol. 15 (1992) 41.
[13] J.A. Spicer, S.A. Gamage, G.J. Finlay, W.A. Denny, Bioorg. Med. Chem. 10 (2002) 19.
[14] T. Takada, K. Kawai, S. Tojo, T. Majima, J. Phys. Chem. B 108 (2004) 761.
[15] F. Cosnard, V. Wintgens, Tetrahedron Lett. 39 (1998) 2751.
[16] C.G. Niu, Z.Z. Li, X.B. Zhang, W.Q. Lin, G.L. Shen, R.Q. Yu, Anal. Bioanal. Chem. 372 (2002) 519.
[17] M.E. Vazquez, J.B. Blanco, B. Imperiali, J. Am. Chem. Soc. 127 (2005) 1300.
[18] A. Demeter, T. Bérces, L. Biczók, V. Wintgens, P. Valat, J. Kossanyi, J. Phys. Chem. 100 (1996) 2001.
[19] V. Wintgens, P. Valat, J. Kossanyi, A. Demeter, L. Biczók, T. Bérces, J. Photochem. Photobiol. A Chem. 93 (1996) 109.
[20] A. Demeter, T. Bérces, L. Biczók, V. Wintgens, P. Valat, J. Kossanyi, J. Chem. Soc. Faraday Trans. 90 (1994) 2635.
[21] H. Cao, V. Chang, R. Hernandez, M.D. Heagy, J. Org. Chem. 70 (2005) 4929.
[22] P. Valat, V. Wintgens, J. Kossanyi, L. Biczók, A. Demeter, T. Bérces, Helvetica Chim. Acta 84 (2001) 2813.
[23] P. Valat, V. Wintgens, J. Kossanyi, L. Biczók, A. Demeter, T. Bérces, J. Am. Chem. Soc. 114 (1992) 946.
[24] G.H. Bon Hoa, J. Kossanyi, A. Demeter, L. Biczók, T. Bérces, Photochem. Photobiol. Sci. 3 (2004) 473.
[25] H. Cao, T. McGill, M.D. Heagy, J. Org. Chem. 69 (2004) 2959.
[26] W.R. Abrams, R.G. Kallen, J. Am. Chem. Soc. 98 (1976) 7777.
[27] D.F. Eaton, Pure Appl. Chem. 60 (1988) 1107.
[28] L. Biczók, T. Bérces, H. Inoue, J. Phys. Chem. A 103 (1999) 3837.
[29] M.J. Frisch, G.W. Trucks, H.B. Schlegel, G.E. Scuseria, M.A. Robb, J.R. Cheeseman, J.A. Montgomery Jr., T. Vreven, K.N. Kudin, J.C. Burant, J.M. Millam, S.S. Iyengar, J. Tomasi, V. Barone, B. Mennucci, M. Cossi, G. Scalmani, N. Rega, G.A. Petersson, H. Nakatsuji, M. Hada, M. Ehara, K. Toyota, R. Fukuda, J. Hasegawa, M. Ishida, T. Nakajima, Y. Honda, O. Kitao, H. Nakai, M. Klene, X. Li, J.E. Knox, H.P. Hratchian, J.B. Cross, C. Adamo, J. Jaramillo, R. Gomperts, R.E. Stratmann, O. Yazyev, A.J. Austin, R. Cammi, C. Pomelli, J.W. Ochterski, P.Y. Ayala, K. Morokuma, G.A. Voth, P. Salvador, J.J. Dannenberg, V.G. Zakrzewski, S. Dapprich, A.D. Daniels, M.C. Strain, O. Farkas, D.K. Malick, D. Rabuck, K. Raghavachari, J.B. Foresman, J.V. Ortiz, Q. Cui, A.G. Baboul, S. Clifford, J. Cioslowski, B.B. Stefanov, G. Liu, A. Liashenko, P. Piskorz, I. Komaromi, R.L. Martin, D.J. Fox, T. Keith, M.A. Al-Laham, C.Y. Peng, A. Nanayakkara, M. Challacombe, P.M.W. Gill, B. Johnson, W. Chen, M.W. Wong, C. Gonzalez, J.A. Pople, Gaussian 03, Revision B. 05, Gaussian Inc., Pittsburgh, PA, 2003.
[30] Neese, F. ORCA, An Ab Initio, Density Functional and Semiempirical Program Package, version 2.4, Max-Planck-Institut für Bioanorganische Chemie, Mülheim an der Ruhr, 2004.
[31] E.M. Kosower, J. Am. Chem. Soc. 80 (1958) 3261.
[32] S.L. Murov, G.L. Carmichael, I. Hug, Handbook of Photochemistry, second ed., Marcell Dekker, New York, 1993.
[33] V. Wintgens, P. Valat, J. Kossanyi, L. Biczók, A. Demeter, T. Bérces, J. Chem. Soc. Faraday Trans. 90 (1994) 411.
[34] E.C. Lim, J. Phys. Chem. 90 (1986) 6770.
[35] I.R. Gould, R.H. Young, L.J. Mueller, A.C. Albrecht, S. Farid, J. Am. Chem. Soc. 116 (1994) 3147.
[36] I.R. Gould, D. Noukakis, L. Gomez-Jahn, R.H. Young, J.L. Goodman, S. Farid, Chem. Phys. 176 (1993) 439.